ORIGINAL PAPER

Caloforines A–G, coumarins from the bark of *Calophyllum scriblitifolium*

Ai Ogasawara[1] · Ryo Noguchi[1] · Takuya Shigi[1] · Alfarius Eko Nugroho[1] · Yusuke Hirasawa[1] · Toshio Kaneda[1] · Takahiro Tougan[2] · Toshihiro Horii[3] · A. Hamid A. Hadi[4] · Hiroshi Morita[1]

Abstract

Bioactivity-guided separation of the methanol extract of *Calophyllum scriblitifolium* bark led to the isolation of five new pyranocoumarins, caloforines A–E (**1–5**) and two new coumarins, caloforines F and G (**6** and **7**). Their structures were elucidated by 1D and 2D NMR spectroscopy, and their absolute configurations were investigated by a combination of CD spectroscopy and DFT calculation. Caloforines A–F (**1–6**) showed moderate antimalarial activity against *Plasmodium falciparum* 3D7 strain.

Graphical abstract
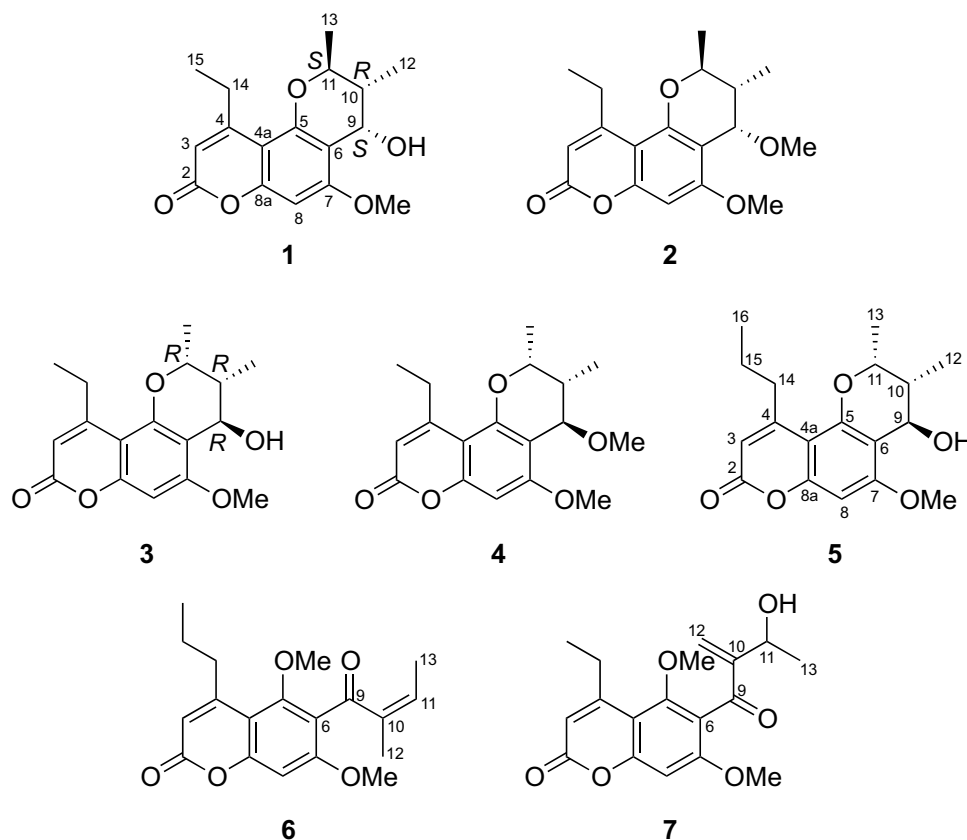
Extended author information available on the last page of the article

Introduction

Malaria is the largest parasitic protozoan infection in humankind in which malaria infects humans through the anopheles mosquito. Malaria is not only widespread throughout the tropics but also occurs in many temperate regions. In light of this problem, scientists have turned to naturally occurring compounds obtained from plants recurrently used in traditional medicine [1]. As part of our ongoing effort to isolate and identify novel antimalarial natural products from a variety of natural sources, our laboratory reported the discovery of various types of skeletal natural products showing antimalarial activity [2–8].

Calophyllum, the largest genus in the Calophyllaceae family, is composed of over 200 species distributed mainly in the tropical region [9]. Plants of this genus have been reported for several ethnomedicinal uses in the traditional systems of medicine [10]. In addition, plants of this genus have been reported to contain xanthones, flavonoids, acylphloroglucinols, terpenoids and chromanones [11, 12]. The scientific study of the genus *Calophyllum* revealed that it is a rich source of bioactive secondary metabolites showing a wide range of biological activities. Some coumarins from *C. flavoranulum* showed activity against *Plasmodium berghei* parasite [13].

We have reported *Calophyllum* chromanones (calofolic acids A–F) showing dose-dependent vasorelaxation activity on isolated rat aorta, have been isolated from the tropical tree *C. scriblitifolium* [14]. In our search for new bioactive compounds, we investigated the MeOH extract of *C. scriblitifolium* which showed antimalarial activity. Bioactivity-guided separation of the extract led to the isolation of five new pyranocoumarins, caloforines A–E (**1–5**) and two new coumarins, caloforines F and G (**6** and **7**) (Fig. 1). Structure elucidation of **1–7** and the antimalarial activity of the isolated coumarins, caloforines A–F (**1–6**) are reported herein.

Results and discussions

Caloforine A (**1**) was obtained as an optically active colorless amorphous solid, − 40 (*c* 1.0, MeOH) and revealed to have the molecular formula $C_{17}H_{20}O_5$, requiring eight degrees of unsaturation, by HRESIMS. The IR spectrum showed an important absorption at 1717 cm^{-1} for the unsaturated ester carbonyl group. The UV spectrum (λ_{max} 221, 232, 259, and 321 nm) indicated the presence of a coumarin chromophore. The ^{1}H and ^{13}C NMR data (Tables 1 and 3) and HSQC spectrum of **1** revealed the presence of seventeen carbon signals due to three *sp³* methines, one *sp³* methylene,
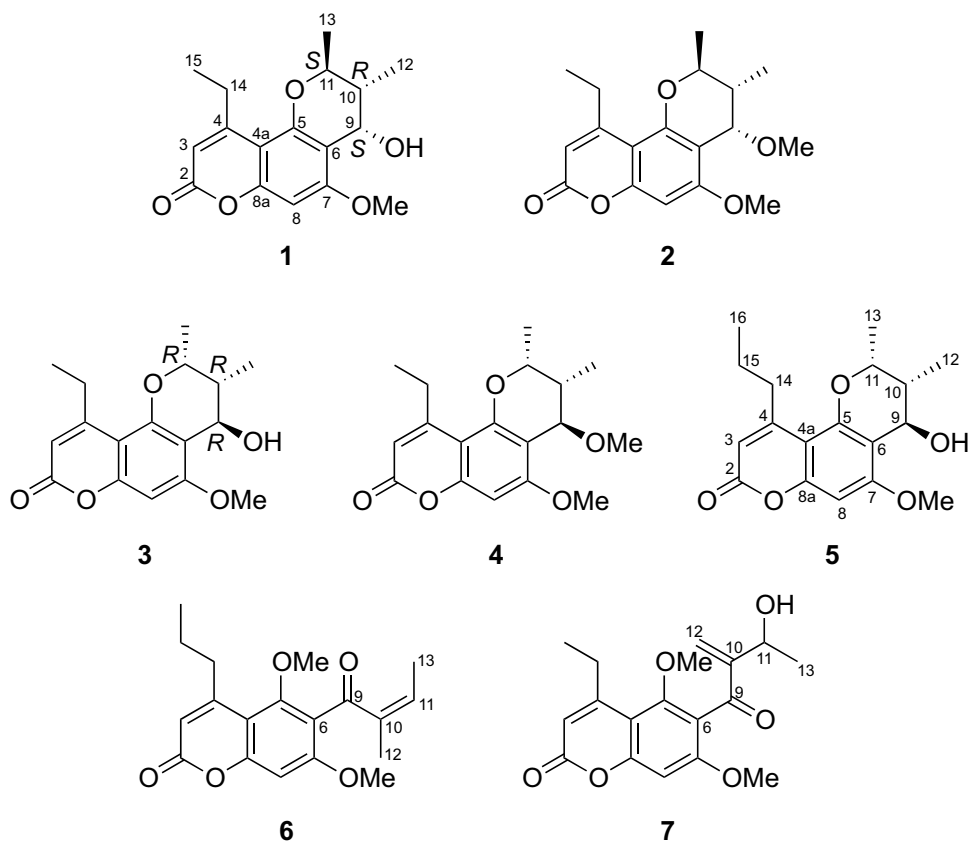
Fig. 1 Structures of **1–7**

Table 1 ¹H NMR data of **1–7** in CDCl₃

No	1	2	3	4
3	5.99 (s)	5.97 (s)	6.01 (s)	5.98 (s)
8	6.43 (s)	6.42 (s)	6.47 (s)	6.42 (s)
9	4.78 (d, 3.5)	4.36 (d, 2.8)	4.64 (d, 1.2)	4.15 (d, 1.8)
10	1.74 (dqd, 10.8, 7.1, 3.5)	1.69 (dqd, 12.3, 6.2, 2.8)	2.00 (qdd, 7.3, 1.6, 1.2)	2.03 (qdd, 7.7, 2.0, 1.8)
11	4.20 (dq, 10.8, 6.2)	4.30 (dq, 12.3, 6.6)	4.43 (qd, 6.6, 1.6)	4.47 (qd, 6.7, 2.0)
12	1.15 (d, 7.1)	1.13 (d, 6.6)	0.81 (d, 7.3)	0.76 (d, 7.1)
13	1.45 (d, 6.7)	1.42 (d, 6.2)	1.46 (d, 6.6)	1.45 (d, 6.7)
14	2.97 (m)	2.97 (m)	2.98 (m)	2.97 (m)
15	1.23 (t, 7.5)	1.22 (t, 7.3)	1.23 (t, 7.3)	1.21 (t, 6.8)
7-OMe	3.91 (s)	3.88 (s)	3.92 (s)	3.89 (s)
9-OMe		3.49 (s)		3.45 (s)

No	5	6	7
3	5.98 (s)	6.10 (s)	6.15 (s)
8	6.47 (s)	6.64 (s)	6.65 (s)
9	4.64 (d, 1.8)		
10	2.00 (qdd, 7.3, 1.8, 1.5)		
11	4.42 (qd, 6.5, 1.5)	6.25 (q, 7.5)	4.87 (q, 6.4)
12	0.80 (d, 7.3)	1.82 (d, 7.5)	5.79 (s)
			6.18 (s)
13	1.46 (d, 6.5)	1.92 (s)	1.48 (d, 6.4)
14	2.89 (m)	2.83 (t, 7.6)	2.96 (q, 7.7)
15	1.63 (m)	1.63 (m)	1.26 (t, 7.7)
16	1.01 (t, 7.5)	1.00 (t, 7.5)	
5-OMe		3.71 (s)	3.75 (s)
7-OMe	3.92 (3H, s)	3.79 (s)	3.81 (s)

Fig. 2 Selected 2D NMR correlations of **1**
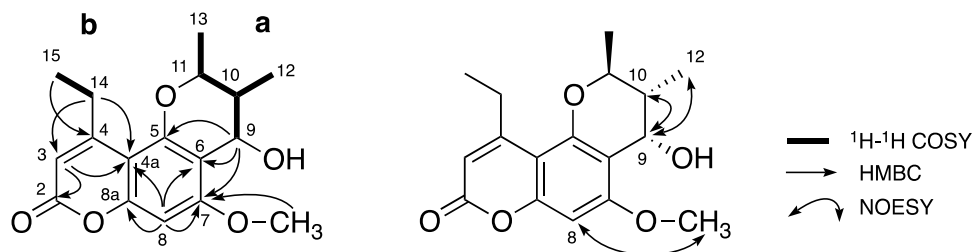
four methyls, seven sp^2 quaternary carbons, and two sp^2 methines. Among them, three sp^2 quaternary carbons (δ_C 153.5, 156.7, and 160.4) and one methyl carbon (δ_C 56.0) were attributed to those attached to an oxygen atom.

The gross structure of **1** was elucidated by analysis of 2D NMR data including the ¹H-¹H COSY, HSQC, and HMBC spectra. Analyses of the HSQC and ¹H-¹H COSY spectra revealed the presence of two partial structures; **a** (C-9~C-13) and **b** (C-14~C-15). The connections between two partial structures and coumarin skeleton were deduced mainly from the HMBC correlations of H-9, H₂-14, and H₃-15 (Fig. 2). In addition, the presence of a methoxy group at C-7 was deduced from the HMBC correlations of OCH₃-7, H-8 and H-9 to C-7. Thus, **1** was revealed as a tetrahydropyranoyl coumarin as

shown in Fig. 1, which may be derived from tiglyl moiety at C-6, with an ethyl group at C-4 and a methoxy group at C-7.

The relative stereochemistry of C-9, C-10, and C-11 was elucidated from ^3J coupling constants as in the case of those of calanolides from *Calophyllum lanigerum* [15]. The $^3J_{H10-H11}$ constant (10.8 Hz) indicated *anti* relation between H-10 and H-11, whereas that of $^3J_{H9-H10}$ (3.5 Hz) *syn* relation between H-9 and H-10.

Caloforine B (**2**) was determined to have the molecular formula, $C_{18}H_{22}O_5$ which was larger than that of **1** by a CH₂ unit. The ¹H and ¹³C NMR data are highly similar and the presence of a methoxy group (δ_H 3.49) at C-9, indicating the structure of **2** as 9-methoxy caloforine A. Analysis of the 2D NMR data further supported the proposed structure (Fig. 3).

In particular, the HMBC correlation of the methoxymethyl to C-9 confirmed the position of the methoxy group at C-9. The same relative stereochemistry of C-9, C-10, and C-11 as **1** was elucidated from ^3J coupling constants ($^3J_{H10-H11}$ 12.3 Hz and $^3J_{H9-H10}$ 2.8 Hz) as in the case of those of **1**.

The molecular formulae of caloforines C (**3**) and D (**4**) were also determined to be $C_{17}H_{20}O_5$ and $C_{18}H_{22}O_5$, respectively, as those of **1** and **2**. Furthermore, their NMR data are also highly similar to **1** and **2**, respectively. However, ^3J coupling constants of the signals associated with H-9 – H-11 were different from those of **1** and **2**. The $^3J_{H10-H11}$ constant (1.6 Hz) indicated *syn* relation between H-10 and

H-11, whereas that of $^3J_{H9-H10}$ (1.2 Hz) *syn* relation between H-9 and H-10 [15]. Analysis of the 2D NMR data (Fig. 4) supported the structures of **3** and **4** to be as shown in Fig. 1. Each stable conformer of **1** and **3** was shown in Fig. 5 to clarify the relationship of $^3J_{H-H}$ coupling constants associated with H-9 – H-11 (*syn* and *anti* relation).

Caloforine E (**5**) was revealed to have the molecular formula $C_{18}H_{22}O_5$ by HRESIMS. It's NMR data are highly similar to **3**. However, the signals [(δ_H 2.98 (2H, m) and 1.23 (3H, t, 7.3)] for ethyl group at C-4 in **3** are not observed in **5**, and a propyl signal [(δ_H 2.90 (2H, m), 1.65 (2H, m), and 1.05 (3H, t, 7.5)]

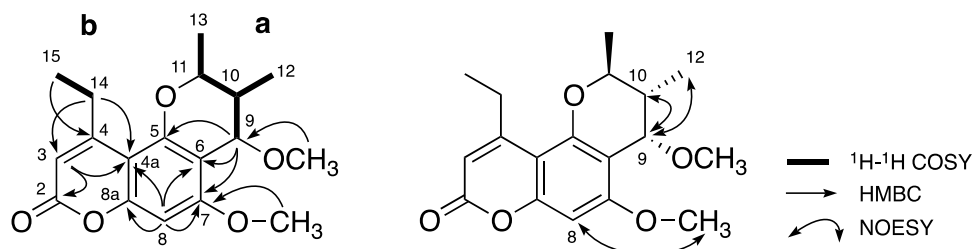**Fig. 3** Selected 2D NMR correlations of **2**

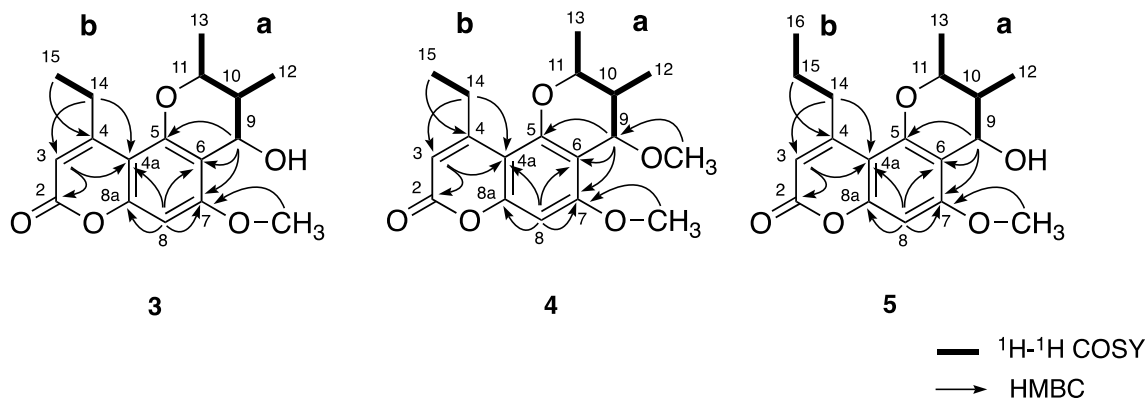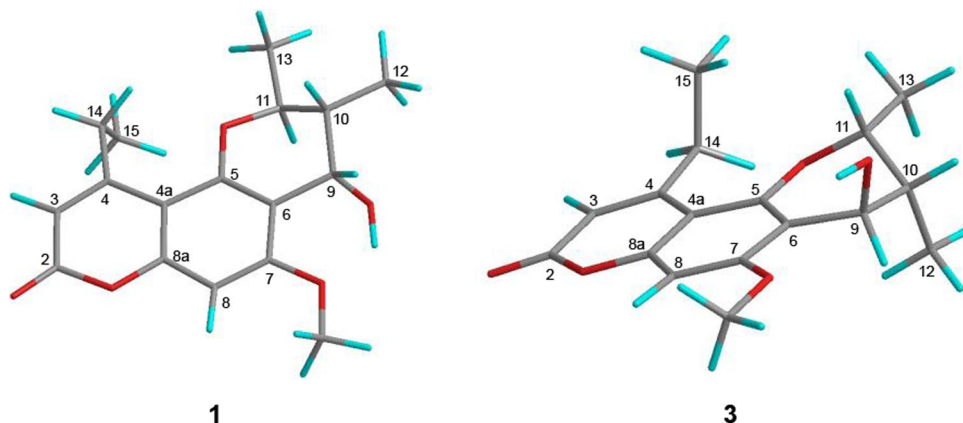**Fig. 4** Selected 2D NMR correlations of **3**, **4** and **5**

Fig. 5 Stable conformers of **1** and **3**

are observed instead. The proposed structure as shown in Fig. 1 was confirmed through analysis of the 2D NMR data (Fig. 4).

Electronic circular dichroism (ECD) may provide a powerful approach to the determination of the absolute configuration of natural products [16]. The absolute configuration of caloforines A–E (**1**–**5**) was assigned by comparing the experimental CD spectra shown in Fig. 6 and the calculated CD spectra. CD calculation was performed by Turbomole 7.1 [17] using RI-TD-DFT-B3LYP/def2-SVPD level of theory on RI-DFT-B3LYP/def2-SVP optimized geometries. The experimental CD spectra show a similar CD pattern compared to calculated CD spectra (Fig. 6). Therefore, the absolute configuration of caloforines A and B (**1** and **2**) was proposed to be 9*S*, 10*R*, 11*S* and that of caloforines C–E (**3**–**5**) 9*R*, 10*R*, 11*R* as shown in Fig. 1.

Caloforine F (**6**) was revealed to have the molecular formula $C_{19}H_{22}O_5$ by HRESIMS. The IR spectrum showed two absorptions at 1735 and 1660 cm^{-1} for unsaturated ester carbonyl and unsaturated ketone groups, respectively. The UV spectrum (λ_{max} 226, 242, and 322 nm) indicated the presence of a coumarin chromophore.
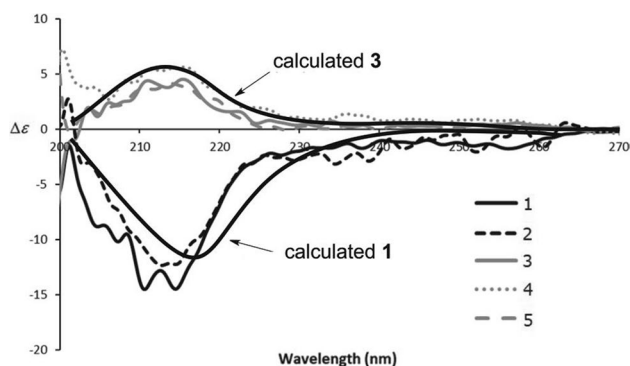

Fig. 6 Experimental and calculated CD spectra of **1**–**5**

Table 2 Antimalarial activity against *P. falciparum* 3D7 of **1**–**7**

	IC$_{50}$ (μM)
1	23.5
2	20.3
3	25.9
4	9.4
5	35.5
6	25.3
7	> 50 (GI = 14.7% at 50 μM)

The ^{1}H and ^{13}C NMR data (Tables 1 and 3) and HSQC spectrum of **6** revealed the presence of nineteen carbon signals due to one ketone, one ester ketone, two methoxyls, two sp^3 methylenes, three methyls, three sp^2 methines, and seven sp^2 quaternary carbons. Among them, three sp^2 quaternary carbons (δ_C 155.8 156.7, and 159.4) and two methyl carbons (δ_C 56.3 and 63.7) were attributed to those attached to an oxygen atom.

The gross structure of **6** was elucidated by analysis of 2D NMR data including the ^{1}H-^{1}H COSY, HSQC, and HMBC spectra (Fig. 7). Analyses of the HSQC and ^{1}H-^{1}H COSY spectra revealed the presence of two partial structures; **a** (C-11 ~ C-12) and **b** (C-14 ~ C-16). The connections between the partial structure **a** and a coumarin skeleton were deduced mainly from the HMBC correlations of H-14 and H$_2$-15. In addition, the presence of a methoxy group at C-5 and C-7 was deduced from the NOESY correlation between OCH$_3$-5 and H$_2$-14, and the HMBC correlations of OCH$_3$-7 and H-8 to C-7. Thus, **6** was revealed as a coumarin with a propyl group at C-4, an angelyl moiety at C-6, and two methoxy groups at C-5 and C-7.

Caloforine G (**7**) was revealed to have the molecular formula $C_{18}H_{20}O_6$ by HRESIMS. The IR spectrum showed two absorptions at 1731 and 1662 cm^{-1} for unsaturated ester carbonyl and unsaturated ketone groups, respectively. Furthermore, the NMR data of **6** and **7** are highly similar to each other. However, the signals associated with the angelyl moiety in **6** is not observed in **7**, and sp^2 methylene and an oxygen-bearing doublet methyl signals (δ_C 128.3, δ_H 5.79 and 6.18, and δ_C 22.2, δ_H 1.48 and δ_C 66.5, δ_H 4.87 for **7**) are observed instead. Furthermore, an ethyl signal instead of a propyl at C-4 is also observed. Therefore, **7** should have a 3-hydroxy-2-methylenebutanoyl moiety instead of an angelyl moiety. Analysis of the 2D NMR data (Fig. 7) supported the structure of **6** and **7** to be as shown in Fig. 1. Caloforine G (**7**), which was considered to be racemate, showed no optical rotation.

Coumarins, which exhibited various biological properties such as antimicrobial, anti-inflammatory, enzyme inhibitory properties, and so on, also displayed potential in vitro anti-plasmodial and in vivo antimalarial activities [18, 19]. Moreover, many of coumarin derivatives. have already been used in clinical practice for the treatment of several diseases.

Caloforines A–G (**1**–**7**) were tested for the antimalarial activity against *P. falciparum* 3D7 strain. The result showed that most of them showed moderate in vitro antimalarial activity [the half-maximal (50%) inhibitory concentration (IC$_{50}$) = 9.4 ~ 35.5 μM, respectively.] (Table 2), whereas **7** did not (> 50 μM). The activity for pyranocoumarins **1**–**5**

Table 3 ^{13}C NMR data of **1–7** in CDCl$_3$

No	1	2	3	4	5	6	7
2	161.4	161.5	161.3	161.4	161.3	160.6	159.4
3	110.2	109.8	110.2	109.9	111.2	112.2	111.5
4	160.2	160.5	160.1	160.2	160.2	157.0	159.4
4a	103.6	103.6	103.6	103.2	103.2	107.1	107.4
5	153.5	153.6	153.6	153.8	152.8	155.8	158.3
6	110.0	108.5	107.3	109.2	106.7	120.4	119.5
7	160.4	160.3	161.3	160.2	161.6	159.4	196.3
8	92.0	91.6	92.3	92.2	92.3	96.0	96.2
8a	156.7	156.8	156.7	156.9	156.8	156.7	158.3
9	62.4	71.0	65.6	73.8	65.6	195.4	196.1
10	37.8	38.0	36.4	33.0	36.4	137.7	153.3
11	73.0	73.3	71.3	70.8	71.3	138.7	66.5
12	12.0	13.0	9.1	9.0	9.1	20.8	128.3
13	18.6	19.0	14.1	17.6	17.6	15.5	22.2
14	29.5	29.6	29.7	29.7	38.8	37.0	27.7
15	14.0	14.0	14.0	14.1	23.2	22.4	13.1
16					13.9	14.0	
5-OMe						63.7	64.0
7-OMe	56.0	56.0	56.0	56.0	56.0	56.3	56.3
9-OMe		59.1		56.6			

might be not influenced by their stereochemistry and substituent patterns.

Experimental section

General experimental procedures

Optical rotations were measured on a JASCO DIP-1000 polarimeter. UV spectra were recorded on a Shimadzu UVmini-1240 spectrophotometer and IR spectra on a JASCO FT/IR-4100 spectrophotometer. CD spectra were recorded on a JASCO J-820 polarimeter. High-resolution ESI MS was obtained on a JMS-T100LP (JEOL). ^{1}H and 2D NMR spectra were measured on a 400 MHz or 600 MHz spectrometer at 300 K, while ^{13}C NMR spectra were on a 100 MHz or 150 MHz spectrometer. The residual solvent peaks were used as internal standard (δ_H 7.26 and δ_C 77.0

for CDCl$_3$). Standard pulse sequences were used for the 2D NMR experiments.
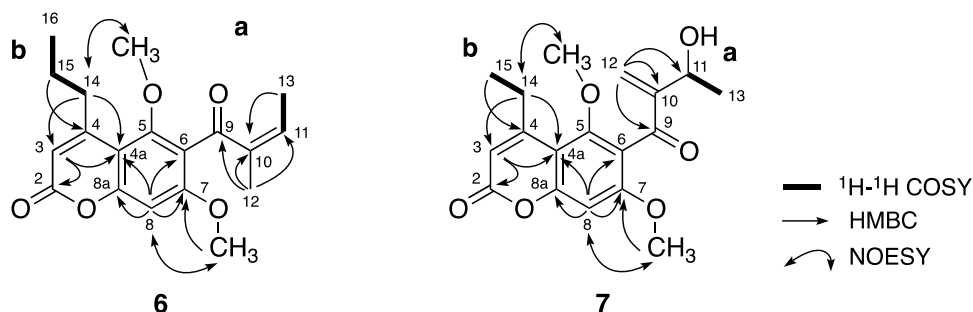
Material

The barks of *C. scriblitifolium* were collected in Mersing, Malaysia in July 2013. The botanical identification was made by Mr. Sani Miran, Herbarium of Universiti Kebangsaan Malaysia. Voucher specimens (Herbarium No. SM2299) are deposited in the Herbarium of Universiti Kebangsaan Malaysia.

Extraction and isolation

The barks of *C. scriblitifolium* (1.0 kg) were extracted with MeOH to obtain 130.8 g of extract. A part of the MeOH extract (50 g) was successively partitioned with

Fig. 7 Selected 2D NMR correlations of **6** and **7**

n-hexane, EtOAc, *n*-BuOH and water. The EtOAc and *n*-BuOH-soluble materials were combined (25.5 g), and further separated by HP-20 column chromatography (H$_2$O/MeOH 1:0 → 4:1 → 3:2 → 1:4 → 0:1, 100% Acetone) to obtain 3 fractions (eb-1–3). The third fraction (eb-3, 1.1 g) was further separated with a silica gel column (Hexane/EtOAc 1:0 → 9:1 → 4:1 → 7:3 → 6:4, CHCl$_3$/MeOH 0:1 → 50:1 → 30:1 → 10:1 → 0:1) to obtain 8 fractions (eb-3–1–7). Further separation of the fraction elucted by Hexane/EtOAc 1:0 → 9:1, by ODS HPLC (Nacalai tesque Cosmosil MS-II, 10 × 250 mm, 70% MeOH at 4.7 mL/min, UV detection at 254 nm) yielded caloforines A (**1**, 0.7 mg, 0.0007%, t_R 56.4 min), B (**2**, 1.1 mg, 0.0011%, t_R 55.6 min), C (**3**, 2.5 mg, 0.0008%, t_R 59.7 min), D (**4**, 0.8 mg, 0.0008%, t_R 58.6 min), E (**5**, 0.9 mg, 0.0011%, t_R 54.8 min), F (**6**, 0.4 mg, 0.0004%, t_R 57.9 min), and G (**7**, 1.0 mg, 0.0010%, t_R 54.6 min).

Caloforine A (**1**): white amorphous solid; − 40 (*c* 1.0, MeOH); IR (film) v_{max} 3447, 2971, 2931, 1717, 1604 cm^{-1}; UV (MeOH) λ_{max} 221 (ε 44,354), 232 (17,146), 259 (7782), 321 (16,538) nm; CD (MeOH) λ_{max} 215 ($\Delta\varepsilon$ -14.3) nm; ^{1}H and ^{13}C NMR data, see Tables 1 and 3; ESIMS *m/z* 327 (M + H)$^+$. HRESIMS *m/z* 305.1387 [calcd for C$_{17}$H$_{21}$O$_5$ (M + H)$^+$: 305.1389].

Caloforine B (**2**): white amorphous solid; − 63 (*c* 1.0, MeOH); IR (film) v_{max} 3465, 2954, 1731, 1699, 1605 cm^{-1}; UV (MeOH) λ_{max} 212 (ε 34,121), 236 (12,434), 259 (5819), 324 (12,561) nm; CD (MeOH) λ_{max} 213 ($\Delta\varepsilon$ -12.33) nm; ^{1}H and ^{13}C NMR data, see Tables 1 and 3; ESIMS *m/z* 319 (M + H)$^+$. HRESIMS *m/z* 319.1552 [calcd for C$_{18}$H$_{23}$O$_5$ (M + H)$^+$: 319.1545].

Caloforine C (**3**): white amorphous solid; + 30 (*c* 1.0, MeOH); IR (film) v_{max} 3447, 2966, 2924,1727, 1604 cm^{-1}; UV (MeOH) λ_{max} 207 (ε 9587), 232 (8404), 259 (4676), 321 (6834) nm; CD (MeOH) λ_{max} 213 ($\Delta\varepsilon$ 3.77) nm; ^{1}H and ^{13}C NMR data, see Tables 1 and 3; ESIMS *m/z* 305 (M + H)$^+$. HRESIMS *m/z* 305.1392 [calcd for C$_{17}$H$_{21}$O$_5$ (M + H)$^+$: 305.1389].

Caloforine D (**4**): white amorphous solid; + 16 (*c* 1.0, MeOH); IR (film) v_{max} 3465, 2964, 1731, 1604 cm^{-1}; UV (MeOH) λ_{max} 232 (ε 27,280), 259 (12,003), 323 (5286), 343 (7570) nm; CD (MeOH) λ_{max} 216 ($\Delta\varepsilon$ 5.62) nm; ^{1}H and ^{13}C NMR data, see Tables 1 and 3; ESIMS *m/z* 319 (M + H)$^+$. HRESIMS *m/z* 319.1545 [calcd for C$_{18}$H$_{23}$O$_5$ (M + H)$^+$: 319.1545].

Caloforine E (**5**): white amorphous solid; + 20 (*c* 1.0, MeOH); IR (film) v_{max} 2925, 1731, 1657, 1604 cm^{-1}; UV (MeOH) λ_{max} 206 (ε 21,415), 233 (8696), 259 (4263), 323 (6188) nm; CD (MeOH) λ_{max} 214 ($\Delta\varepsilon$ 4.14) nm; ^{1}H and ^{13}C NMR data, see Tables 1 and 3; ESIMS *m/z* 319 (M + H)$^+$. HRESIMS *m/z* 319.1544 [calcd for C$_{18}$H$_{23}$O$_5$ (M + H)$^+$: 319.1545].

Caloforine F (**6**): white amorphous solid; IR (film) v_{max} 2924, 1735, 1660 cm^{-1}; UV (MeOH) λ_{max} 206 (ε 24,031), 226 (11,585), 242 (8474), 322 (6984) nm; ^{1}H and ^{13}C NMR data, see Tables 1 and 3; ESIMS *m/z* 331 (M + H)$^+$. HRESIMS *m/z* 331.1548 [calcd for C$_{19}$H$_{23}$O$_5$ (M + H)$^+$: 331.1545].

Caloforine G (**7**): white amorphous solid; IR (film) v_{max} 2961, 1731, 1662, 1602 cm^{-1}; UV (MeOH) λ_{max} 205 (ε 29,797), 223 (15,842), 320 (5019) nm; ^{1}H and ^{13}C NMR data, see Tables 1 and 3; ESIMS *m/z* 333 (M + H)$^+$. HRESIMS *m/z* 333.1350 [calcd for C$_{18}$H$_{21}$O$_6$ (M + H)$^+$: 333.1338].

CD calculation

The conformations were obtained using Monte Carlo analysis with MMFF94 force field and charges on Macromodel 9.1. CD calculations were performed in Turbomole 7.1 using RI-TD-DFT-B3LYP/def2-SVPD level of theory on RI-DFT-B3LYP/def2-SVP optimized geometries [17].

Parasite strain culture

P. falciparum laboratory strain 3D7 was obtained from Prof. Masatsugu Kimura (Osaka City University, Osaka, Japan). For the assessment of antimalarial activity of the compounds in vitro, the parasites were cultured in Roswell Park Memorial Institute (RPMI) 1640 medium supplemented with 0.5 g/L L-glutamine, 5.96 g/L HEPES, 2 g/L sodium bicarbonate (NaHCO$_3$), 50 mg/L hypoxanthine, 10 mg/L gentamicin, 10% heat-inactivated human serum, and red blood cells (RBCs) at a 3% hematocrit in an atmosphere of 5% CO$_2$, 5% O$_2$, and 90% N$_2$ at 37 °C as previously described [20]. Ring-form parasites were collected using the sorbitol synchronization technique [21]. Briefly, the cultured parasites were collected by centrifugation at 840 g for 5 min at room temperature, suspended in a fivefold volume of 5% D-sorbitol (Nacalai Tesque, Kyoto, Japan) for 10 min at room temperature, and then they were washed twice with RPMI 1640 medium to remove the D-sorbitol. The utilization of blood samples of healthy Japanese volunteers for the parasite culture was approved by the institutional review committee of the Research Institute for Microbial Diseases (RIMD), Osaka University (approval number: 22–3).

Antimalarial activity

Ring-form-synchronized parasites were cultured with compounds **1**–**7** at sequentially decreasing concentrations (50, 15, 5, 1.5, 0.5, and 0.15 μM) for 48 h for the flow cytometric analysis using an automated hematology analyzer, XN-30. The XN-30 analyzer was equipped with a prototype algorithm for cultured falciparum parasites (prototype;

software version: 01–03, (build 16)) and used specific reagents (CELLPACK DCL, SULFOLYSER, Lysercell M, and Fluorocell M) (Sysmex, Kobe, Japan) [22, 23]. Approximately 100 μL of the culture suspension diluted with 100 μL phosphate-buffered saline was added to a BD Microtainer MAP Microtube for Automated Process K_2 EDTA 1.0 mg tube (Becton Dickinson and Co., Franklin Lakes, NJ, USA) and loaded onto the XN-30 analyzer with an auto-sampler as described in the instrument manual (Sysmex). The parasitemia (MI-RBC%) was automatically reported [22]. Then 0.5% DMSO alone or containing 5 μM artemisinin was used as the negative and positive controls, respectively. The growth inhibition (GI) rate was calculated from the MI-RBC% according to the following equation:

$$
\begin{aligned}
GI~(\%) =~&100 - (\text{test sample} - \text{positive control}) \\
&/(\text{negative control} - \text{positive control}) \\
&\times 100
\end{aligned}
$$

The IC_{50} was calculated from GI (%) using GraphPad Prism version 5.0 (GraphPad Prism Software, San Diego, CA, USA) [24].

References

1. Wiesner J, Ortmann R, Jomaa H, Schlitzer M (2003) New antimalarial drugs. Angew Chem Int Ed 42:5274–5293
2. Tang Y, Nugroho AE, Hirasawa Y, Tougan T, Horii T, Hadi AHA, Morita H (2019) Leucophyllinines A and B, bisindole alkaloids from *Leuconotis eugeniifolia*. J Nat Med 73:533–540
3. Amelia P, Nugroho AE, Hirasawa Y, Kaneda T, Tougan T, Horii T, Morita H (2019) Indole alkaloids from *Tabernaemontana macrocarpa* Jack. J Nat Med 73:820–825
4. Nugroho AE, Hirasawa Y, Kaneda T, Shirota O, Matsuno M, Mizukami H, Morita H (2021) Triterpenoids from *Walsura trichostemon*. J Nat Med 75:415–422
5. Nugroho AE, Ono Y, Jin E, Hirasawa Y, Kaneda T, Rahman A, Kusumawati I, Tougan T, Horii T, Zaini NC, Morita H (2021) Bisindole alkaloids from *Voacanga grandifolia* leaves. J Nat Med 75:408–414
6. Amelia P, Nugroho AE, Hirasawa Y, Kaneda T, Tougan T, Horii T, Morita H (2021) Two new bisindole alkaloids from *Tabernaemontana macrocarpa* Jack. J Nat Med 75:633–642
7. Hirasawa Y, Yasuda R, Minami W, Hirata M, Nugroho AE, Tougan T, Uchiyama N, Hakamatsuka T, Horii T, Morita H (2021) Divaricamine A, a new anti-malarial trimeric monoterpenoid indole alkaloid from *Tabernaemontana divaricata*. Tetrahedron Lett 83:153423

8. Nugroho AE, Okabe M, Hirasawa Y, Wong CP, Kaneda T, Tougan T, Horii T, Morita H (2021) A novel trimeric triterpene from *Chisocheton ceramicus* Miq. Natural Product commun. https://doi.org/10.1177/1934578X211053202inpress
9. Stevens PF (1980) A revision of the old world species of *Calophyllum* (Guttiferae). J Arnold Arbor 61:117
10. Gupta S, Gupta P (2020) The genus Calophyllum: review of ethnomedicinal uses, phytochemistry and pharmacology. Bioact Nat Prod Drug Discov. https://doi.org/10.1007/978-981-15-1394-7_5
11. Alarcón AB, Cuesta-Rubio O, Pérez JC, Piccinelli AL, Rastrelli L (2008) Constituents of the cuban endemic species *Calophyllum pinetorum*. J Nat Prod 71:1283–1286
12. Cao S, Low K-N, Glover RP, Crasta SC, Ng S, Buss AD, Butler MS (2006) Sundaicumones A and B, polyprenylated acylphloroglucinol derivatives from *Calophyllum sundaicum* with weak activity against the glucocorticoid receptor. J Nat Prod 69:707–709
13. Abbas J, Syafruddin D (2014) Antiplasmodial evaluation of one compound from *Calophyllum flavoranulum*. Indo J Chem 14:185–191
14. Nugroho AE, Sasaki T, Kaneda T, Hadi AHA, Morita H (2017) Calofolic acids A-F, chromanones from the bark of *Calophyllum scriblitifolium* with vasorelaxation activity. Bioorg Med Chem Lett 27:2124–2128
15. Kashman Y, Gustafson KR, Fuller RW, Cardellina JH II, McMahon JB, Currens MJ, Buckheit RW Jr, Hughes SH, Cragg GM, Boyd MR (1992) The calanolides, a novel HIV-inhibitory class of coumarin derivatives from the tropical rainforest tree, *Calophyllum lanigerum*. J Med Chem 35:2735–2743
16. Nugroho AE, Morita H (2019) Computationally-assisted discovery and structure elucidation of natural products. J Nat Med 73:687–695
17. TURBOMOLE V7.1 (2009) A development of University of Karlsruhe and Forschungszentrum Karlsruhe GmbH, 1987–2007
18. Cebrián-Torrejón G, Spelman K, Leblanc K, Muñoz-Durango K, Gutiérrez ST, Ferreira ME, de Arias AR, Figadère B, Maciuk AFA, Grellier P, Cech NB, Poupon E (2011) The antiplasmodium effects of a traditional South American remedy: *Zanthoxylum chiloperone* var. *angustifolium* against chloroquine resistant and chloroquine sensitive strains of *Plasmodium falciparum*. Braz J Pharmacog 21:652–661
19. Subeki S, Matsuura H, Takahashi K, Yamasaki M, Yamato O, Maede Y, Katakura K, Kobayashi S, Trimurningsih T, Chairul C, Yoshihara T (2005) Anti-babesial and anti-plasmodial compounds from *Phyllanthus niruri*. J Nat Prod 68:537–539
20. Trager W, Jensen JB (1976) Human malaria parasites in continuous culture. Science 193(4254):673–675. https://doi.org/10.1126/science.781840
21. Lambros C, Vanderberg JP (1979) Synchronization of *Plasmodium falciparum* erythrocytic stages in culture. J Parasitol 65:418–420
22. Tougan T, Suzuki Y, Itagaki S, Izuka M, Toya Y, Uchihashi K, Horii T (2018) An automated haematology analyzer XN-30 distinguishes developmental stages of falciparum malaria parasite cultured in vitro. Malar J 17:59. https://doi.org/10.1186/s12936-018-2208-6
23. Toya Y, Tougan T, Horii T, Uchihashi K (2021) Lysercell M enhances the detection of stage-specific Plasmodium-infected red blood cells in the automated hematology analyzer XN-31 prototype. Parasitol Int 80:102206. https://doi.org/10.1016/j.parint.2020.102206
24. Tougan T, Toya Y, Uchihashi K, Horii T (2019) Application of the automated haematology analyzer XN-30 for discovery and development of anti-malarial drugs. Malar J 18:8. https://doi.org/10.1186/s12936-019-2642-0

Authors and Affiliations

Ai Ogasawara[1] · Ryo Noguchi[1] · Takuya Shigi[1] · Alfarius Eko Nugroho[1] · Yusuke Hirasawa[1] · Toshio Kaneda[1] · Takahiro Tougan[2] · Toshihiro Horii[3] · A. Hamid A. Hadi[4] · Hiroshi Morita[1]

✉ Hiroshi Morita
moritah@hoshi.ac.jp

[1] Faculty of Pharmaceutical Sciences, Hoshi University, Ebara 2-4-41 Shinagawa-ku, Tokyo 142-8501, Japan

[2] Research Center for Infectious Disease Control, Research Institute for Microbial Diseases, Osaka University, 3-1 Yamadaoka, Suita, Osaka 565-0871, Japan

[3] Department of Malaria Vaccine Development, Research Institute for Microbial Diseases, Osaka University, 3-1 Yamadaoka, Suita, Osaka 565-0871, Japan

[4] Department of Chemistry, Faculty of Science, University of Malaya, 50603 Kuala Lumpur, Malaysia